

NUMERICAL INVESTIGATION OF STATIONARY AND
 FLUCTUATING VIBRATIONAL CONVECTION MODES
 IN A RECTANGULAR CAVITY WITH VARIABLE
 BOUNDARY TEMPERATURE IN WEIGHTLESSNESS

R. R. Siraev

UDC 536.25

The configuration, amplitude, and evolution of average vibrational-oscillatory flows in a rectangular cavity are determined under weightlessness conditions. The convection mode transition is discussed.

Different nongravitational heat and mass transfer mechanisms under weightlessness conditions have been investigated intensively in recent years. Among them, vibrational thermal convection, the average (secondary) flow occurring in a cavity with a nonisothermal fluid or gas performing oscillations (see [1, 2]), is of indubitable interest. Vibrational convection in a rectangular cavity whose opposite boundaries are maintained at distinct homogeneous temperatures was studied in [3, 4]. The heating mode for which the temperature varied linearly along one of the cavity boundaries (long), which corresponded to experimentally realizable preheating conditions, was examined in [5]. The ambiguity of the stationary modes and the transitions between them were disclosed. Processes in a cavity with preheating of the kind mentioned are considered in this paper in the domain of large values of the vibrational Grashof number when the existence is possible of oscillatory convection modes in addition to the stationary ones.

Let us examine a two-dimensional rectangular domain $0 \leq x \leq L, 0 \leq y \leq H$ filled with fluid. All the domain boundaries are solid. It is assumed that there is no static gravity field. The cavity together with the liquid performs high-frequency vibrations along the y axis. The preheating conditions are the following. The boundaries $x = 0$ and $x = L$ parallel to the vibration axis are maintained at the temperature $T = Ay + \Theta$ and $T = 0$, respectively. Therefore, the temperature difference in the section $y = 0$ equals Θ and grows linearly with the coordinate y . The cavity endfaces $y = 0$ and $y = H$ perpendicular to the vibration axis are heat-insulated.

In the case when the oscillation frequency is sufficiently large, the averaging method utilized in [1, 6] permits a closed system of equations to be obtained that describes the average velocity, temperature, and pressure fields

$$\begin{aligned} \frac{\partial \mathbf{v}'}{\partial t'} + (\mathbf{v}' \nabla) \mathbf{v}' &= -\frac{1}{\rho} \nabla p' + \nu \Delta \mathbf{v}' + \varepsilon (\mathbf{w}' \nabla) (T' \mathbf{n} - \mathbf{w}'), \\ \frac{\partial T'}{\partial t'} + \mathbf{v}' \nabla T' &= \chi \Delta T', \quad T' \mathbf{n} = \mathbf{w}' + \nabla \varphi', \\ \operatorname{div} \mathbf{v}' &= 0, \quad \operatorname{div} \mathbf{w}' = 0; \quad \varepsilon = \frac{1}{2} (\beta b \Omega)^2. \end{aligned} \quad (1)$$

Because the temperature on the boundary is inhomogeneous, and also because of the finiteness of the cavity length, mechanical equilibrium turns out to be impossible (see [1]) and vibrational convection is excited in the fluid filling the cavity. We assume that the fluid performed planar motion. We introduce the stream function of the average and fluctuating motions by the relationships

$$v_x = \frac{\partial \psi}{\partial y}, \quad v_y = -\frac{\partial \psi}{\partial x}, \quad w_x = \frac{\partial F}{\partial y}, \quad w_y = -\frac{\partial F}{\partial x}. \quad (2)$$

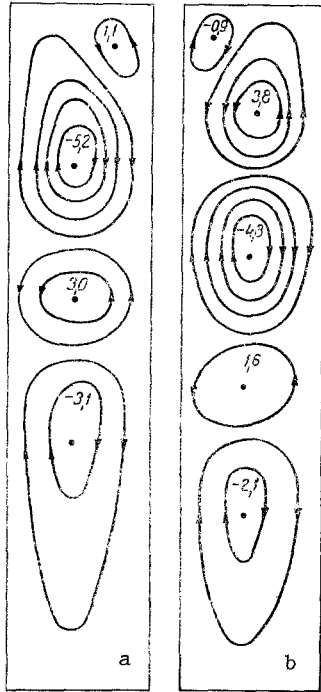


Fig. 1

Fig. 1. Stationary motions for $G = 350$: a) mode 1; b) mode 2.

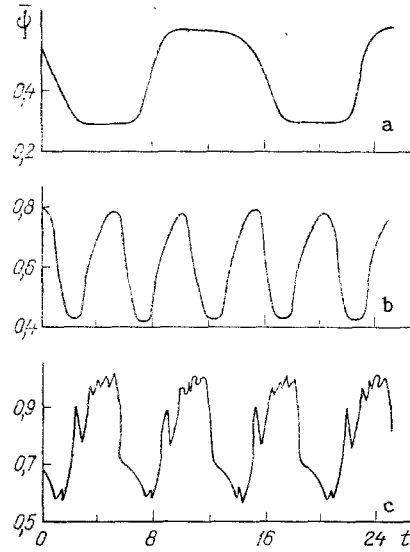


Fig. 2

Fig. 2. Dependence of $\bar{\psi}$ on t for $G = 420$ (a); 700 (b); 1500 (c).

We select L , L^2/ν , ν/L , Θ , respectively, as the units of distance, time, velocity, and temperature. After elimination of the pressure, we obtain a system of plane vibrational convection equations in the dimensionless form

$$\begin{aligned} \frac{\partial}{\partial t} \Delta \psi + D(\psi, \Delta \psi) + GD \left(\frac{\partial F}{\partial x}, T \right) &= \Delta \Delta \psi, \\ \frac{\partial T}{\partial t} + D(\psi, T) &= \frac{1}{P} \Delta T, \quad \Delta F = -\frac{\partial T}{\partial x}, \\ \Delta &= \frac{\partial^2}{\partial x^2} + \frac{\partial^2}{\partial y^2}, \quad D(f, g) = \frac{\partial f}{\partial y} \frac{\partial g}{\partial x} - \frac{\partial f}{\partial x} \frac{\partial g}{\partial y}. \end{aligned} \quad (3)$$

The boundary conditions have the form

$$\begin{aligned} x = 0: \psi &= \frac{\partial \psi}{\partial x} = 0, \quad F = 0, \quad T = 1 + ay; \\ x = 1: \psi &= \frac{\partial \psi}{\partial x} = 0, \quad F = 0, \quad T = 0; \\ y = 0, \quad y = l: \psi &= \frac{\partial \psi}{\partial y} = 0, \quad F = 0, \quad \frac{\partial T}{\partial y} = 0. \end{aligned} \quad (4)$$

The problem is characterized by four dimensionless parameters, the vibrational Grashof number $G = (\beta \Theta L)^2 / 2\nu^2$, the Prandtl number $P = \nu/\chi$, the geometric parameter $\lambda = H/L$ (the ratio between the domain length and width), and the dimensionless temperature gradient on the boundary $a = AL/\Theta$.

The boundary value problem (3) and (4) was solved by finite differences. An explicit scheme of second order accuracy in a 15×30 mesh was used to find the temperature and velocity vortex (see [7, 8]). The stream function fields were calculated by the method of se-

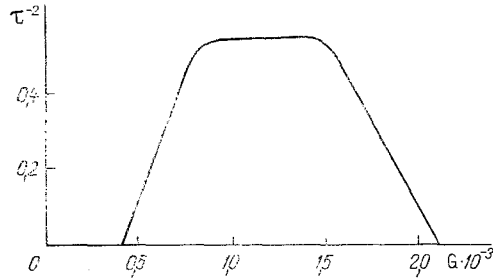


Fig. 3

Fig. 3. Dependence of τ^{-2} on G .

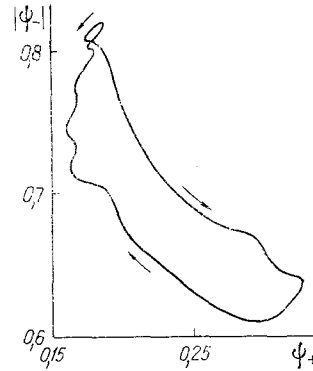


Fig. 4

Fig. 4. Phase trajectory ($G = 420$).

quential upper relaxation. The accuracy of iterating the Poisson equation was 10^{-5} for oscillatory motion computations and 10^{-4} for stationary motion computations. The calculations were performed for the following parameter values: 1) $\ell = 5$, $a = 0.5$; 2) $\ell = 5$, $a = 1$; 3) $\ell = 8$, $a = 1$. The Prandtl number in the computations was fixed: $P = 1$.

The following verification of the method was performed in the nonstationary mode investigations: diminution of the spatial step (computations on a 30×50 mesh), diminution (twofold) of the time step, raising the accuracy of iterating the Poisson equation (to 10^{-6}). The configuration and amplitude of the oscillatory motions were practically invariant here.

Let us examine the results of computations in greater detail for the case $\ell = 5$, $a = 1$. Two stationary motions are realized in the system in the situation under consideration. One is excited by arbitrarily small values of the vibrational Grashof number (mode 1), the other occurs in a threshold manner (mode 2). For small values of G mode 1 is a single-vortex mode. As G increases the motion is rearranged into a three-vortex one in an evolutionary manner (see Fig. 1a). The emergence into mode 2 is realized in a "hard" manner (by giving the perturbation a finite amplitude). This mode occurs for $G \geq 180$; near the threshold the motion has a three-vortex configuration which later becomes a four-vortex one as G grows (see Fig. 1b). The stability domains of the configurations corresponding to modes 1 and 2 overlap in the range of values $180 \leq G \leq 400$.

However, the stationary modes are not those uniquely possible. For $G \geq G_1 = 400$ the stationary motions (modes 1 and 2) become unstable (practically simultaneously in the numerical computation) and regular oscillations (mode 3) occur in the system.

To describe the nonstationary modes we introduce a quantity that is the mean value of the stream function over all the nodes i, j of the computational mesh

$$\bar{\psi} = \frac{1}{K} \sum_{ij} \psi_{ij}$$

(K is the total number of nodes), as well as the quantities ψ_+ and ψ_- that are, respectively, the sum of all the positive and negative values of the stream functions over all the mesh nodes.

The dependence $\bar{\psi}(t)$ is represented in Fig. 2 for different values of the Grashof number (mode 3). As the parameter G increases the amplitude of the oscillations is practically invariant while the period of the oscillations (Fig. 3) and their shape depend substantially on the Grashof number. Three characteristic sections can be isolated in Fig. 3. The quantity τ^{-2} grows in the section $400 \leq G \leq 900$, while the graph of $\bar{\psi}(t)$ has a "step" shape (Fig. 2a). The period of the oscillations in the range $900 \leq G \leq 1500$ retains a constant value while the oscillations acquire an almost sinusoidal shape (Fig. 2b). A further increase in G ($1500 \leq G \leq 2100$) is accompanied by a diminution in the quantity τ^{-2} and the shape of the oscillations is complicated substantially here (Fig. 2c).

The dependence $\tau^{-2}(G)$ permits expressing the proposition about the origination of a cycle from a saddle-node separatrix.

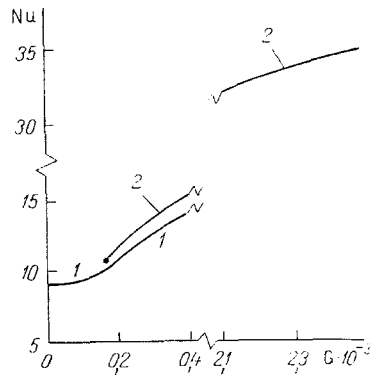


Fig. 5. Dependence of Nu on G for the stationary modes 1 and 2.

The phase trajectory for $G = 420$ is presented in Fig. 4.

For $G \geq 2100$ a stationary mode which is similar to mode 2 in configuration is built up in the system.

We introduce the Nusselt number

$$Nu = \int_0^l \frac{\partial T}{\partial x} dy$$

for the heat flux characteristics in the cavity.

The dependence of Nu on the Grashof number is represented in Fig. 5 for the stationary modes. It is interesting to note the closeness of the mode 1 and 2 heat fluxes in the neighborhood of $G \sim 180$. This is associated with the fact that the total vortex intensities for motions of both kinds are approximately identical for $G \approx 180$. Upon the build up of a nonstationary mode in the system, the heat flux, as all the integral and local flow characteristics also, experiences periodic oscillation.

As computations showed, regular oscillations indeed occur for $\ell = 5$, $a = 0.5$ and $\ell = 8$, $a = 1$.

Therefore, the domain of regular oscillations turns out to be bounded in the Grashof number by stationary motion domains.

NOTATION

x, y , Cartesian coordinates; v, T , and p , average velocity, temperature, and pressure (the primes refer to dimensional quantities); ψ, F , stream functions of the average and fluctuating motions; $w, \nabla\varphi$, solenoidal and irrotation parts of the vector field Tn ; n , unit vector directed along the vibration axis; Ω, b , angular velocity and amplitude of the vibrations; ν , coefficient of kinematic viscosity; χ , temperature diffusivity coefficient; β , thermal expansion coefficient; ρ , density; θ , temperature difference; ℓ , a geometric parameter; P , Prandtl number; G , vibrational Grashof number; a , temperature gradient; τ , period of oscillation; $\bar{\psi}$, average value of the stream function; and Nu , Nusselt number.

LITERATURE CITED

1. G. Z. Gershuni and E. M. Zhukovitskii, Dokl. Akad. Nauk SSSR, 249, No. 3, 580-584 (1979).
2. G. Z. Gershuni and E. M. Zhukovitskii, Hydromechanics and Transport Processes in Weightlessness [in Russian], Sverdlovsk (1984), pp. 86-105.
3. G. Z. Gershuni, E. M. Zhukovitskii, and Yu. S. Yurkov, Izv. Akad. Nauk SSSR, Mekh. Zhidk. Gaza, No. 4, 94-99 (1982).
4. G. Z. Gershuni, E. M. Zhukovitskii, and Yu. S. Yurkov, Viscous Flow Problems [in Russian], Novosibirsk (1981), pp. 19-23.
5. R. R. Siraev, Convective Flows [in Russian], Perm (1987), pp. 55-61.
6. S. M. Zen'kovskaya and I. B. Simonenko, Izv. Akad. Nauk SSSR, Mekh. Zhidk. Gaza, No. 5, 51-55 (1966).
7. E. L. Tarunin, Hydrodynamics [in Russian], Perm (1968), pp. 135-168.
8. E. L. Tarunin, Two-Field Method of Solving Viscous Fluid Hydrodynamics Problems [in Russian], Perm (1985).